



**POLITECNICO**  
MILANO 1863

SCUOLA DI INGEGNERIA INDUSTRIALE  
E DELL'INFORMAZIONE

EXECUTIVE SUMMARY OF THE THESIS

## Systematic tuning of hierarchical attitude controllers with application to UAVs

LAUREA MAGISTRALE IN AERONAUTICAL ENGINEERING - INGEGNERIA AERONAUTICA

**Author:** MICHELE LABORI

**Advisor:** PROF. DAVIDE INVERNIZZI

**Academic year:** 2022-2023

### 1. Introduction

This thesis work deals with the attitude control problem, with specific focus on nonlinear attitude control and its application to multirotor UAV. In this work, a hierarchical architecture based on an inner-outer loop paradigm is considered to simplify the control design, by splitting the problem in kinematic and dynamic attitude control. Nonlinear PID-like controllers are used at the inner loop level to control the angular velocity. Two alternative nonlinear solutions borrowed from the literature are instead exploited in the outer loop for kinematic control. Specifically, the first solution is based on a widely adopted nonlinear stabilizer for full attitude control, which draws inspiration from [2]; this architecture is implemented within a nonlinear geometric filter, as described in [6], to address the computation of the time derivative of the desired attitude to implement feedforward terms without cumbersome analytic derivations. The second solution is based on the geodesic feedback stabilizer proposed in [4], which prioritizes reduced attitude control; this control law has then been modified with respect to [4] incorporate error-dependent variable gains that are found to be beneficial to mitigate saturation effects in multirotor UAVs. Another contribution

of this work is to derive a systematic tuning approach of the gains of the proposed control laws, similar to the  $H_\infty$  synthesis proposed in [3].

### 2. Mathematical modeling

This section quickly reviews the attitude dynamic modeling using a coordinate-free formulation based on rotation matrices and with a specialization to the attitude dynamics of small-scale UAVs.

#### 2.1. Rigid body motion

The configuration of the rigid body is described by the rotation matrix  $R(t) \in SO(3)$ , which is an orthogonal matrix that satisfies:

$$R^T R = I_3 \quad (1)$$

where  $I_3$  is the  $(3 \times 3)$  identity matrix and  $b_i$  are the body axes resolved in the inertial frame. The attitude motion of the rigid body is described by Equation (2) :

$$\begin{cases} \dot{R} = RS(\omega) & (2a) \\ J\dot{\omega} = -S(\omega)J\omega + \tau_c + \tau_e & (2b) \end{cases}$$

where  $J = J^T \in \mathbb{R}_{>0}^{3 \times 3}$  is the inertia matrix expressed in the body frame,  $\omega \in \mathbb{R}^3$  is the body angular velocity,  $\tau_c \in \mathbb{R}^3$  is the control torque

exerted by the actuators and  $\tau_e \in \mathbb{R}^3$  accounts for unknown exogenous effects. The map  $S$  is the map between  $\mathbb{R}^3$  and  $so(3)$ , where it is defined as equation (3):

$$so(3) := \{\Omega \in \mathbb{R}^{3 \times 3} : \Omega = -\Omega^T\}. \quad (3)$$

## 2.2. Quadrotor UAVs

The attitude dynamics of a quadrotor UAV is defined as follows:

$$\begin{cases} \dot{R} = RS(\omega) & (4a) \\ \mathbf{G}(s)\omega = \tau_c + \tau_e & (4b) \end{cases}$$

where  $\mathbf{G}(s)$  is matrix of transfer function, defined as follows:

$$\mathbf{G}(s) = \begin{bmatrix} G_{roll}(s) & 0 & 0 \\ 0 & G_{pitch}(s) & 0 \\ 0 & 0 & G_{yaw}(s) \end{bmatrix} \quad (5)$$

where each element on the diagonal is a model (in the laplace domain) that links the control input ( $\tau_c$ ) with the angular velocity ( $\omega$ ). Such a model can be obtained with physic-based modeling or with black-box identification techniques, e.g., the PBSID algorithm. The linear modeling is justified by the small contribution of gyroscopic terms for small-scale UAVs. Using identification techniques allow capturing additional effects (such as sensor and actuator dynamics) thereby improving the accuracy of the model.

## 3. Hierarchical approach to attitude control

In this section, the proposed attitude control architecture is presented, both for the rigid body and the UAV dynamics.

### 3.1. Rigid Body and UAV Attitude Control

By referring to the model in Equation (2), the objective of the attitude control design is to guarantee attitude tracking in the presence of disturbances. Let the attitude and the angular velocity error coordinates be defined as:

$$\begin{cases} R_e = R_d^T R & (6a) \\ \omega_e = \omega_v - \omega & (6b) \end{cases}$$

Then, consider the following modular hierarchical control law:

$$\begin{cases} \tau_c = S(\omega)J\omega + J\dot{\omega}_v + \gamma_\omega & (7a) \\ \dot{x}_c = \gamma_c(x_c, \omega_e, \omega_v) & (7b) \end{cases}$$

$$\begin{cases} \omega_v = \gamma_R(R_e) + R_e^T \omega_d(t) & (8a) \\ \dot{\omega}_v = \dot{\gamma}_R(R_e) & (8b) \\ -S(\gamma_R(R_e) - \omega_e)R_e^T \omega_d + R_e^T \dot{\omega}_d(t) & (8b) \end{cases}$$

In (7)  $x_c \in \mathbb{R}^{n_c}$  represents the controller state and  $\gamma_R(\cdot) : SO(3) \rightarrow \mathbb{R}^3$ , while  $\gamma_\omega(\cdot, \cdot, \cdot) : \mathbb{R}^{n_c} \times \mathbb{R}^3 \times \mathbb{R}^3 \rightarrow \mathbb{R}^3$ ,  $\gamma_c(\cdot, \cdot, \cdot) : \mathbb{R}^{n_c} \times \mathbb{R}^3 \times \mathbb{R}^3 \rightarrow \mathbb{R}^3$  are continuous stabilizers to be defined. Considering Equations (2) and (7a), using the definitions given by (6), the closed-loop dynamic errors are the following:

$$\begin{cases} \dot{R}_e = R_e S(\gamma_R(R_e) - \omega_e) & (9a) \\ J\dot{\omega}_e = -\gamma_\omega(x_c, \omega_e, \omega_v(R_e, t)) - \tau_e & (9b) \\ \dot{x}_c = \gamma_c(x_c, \omega_e, \omega_v(R_e, t)) & (9c) \end{cases}$$

The outer loop stabilizer function is defined as  $\gamma_R(R_e) = -S^{-1}(skew(K_r R_e))$  where  $K_r \in \mathbb{R}^{3 \times 3}$  is a symmetric matrix with distinct eigenvalues satisfying  $tr(K_r)I_3 - K_r \in \mathbb{R}_{>0}^{3 \times 3}$ . The proposed inner loop stabilizer function is:

$$\begin{cases} \gamma_c = A_c x_c + B_c \omega_e & (10a) \\ \gamma_\omega = C_c x_c + (D_c + K_\omega) \omega_e & (10b) \\ + S(\omega_e)J(\omega_v - \omega_e) \end{cases}$$

The inner loop (Equations (7a) and (7b)) is in charge of assigning a suitable control torque  $\tau_c$  to track the angular velocity reference  $\omega_v$  provided by the outer loop (Equations (8a) and (8b)). Equation (7b) is used to resume a behaviour similar to a PID controller.

Regarding the UAV controller, the outer loop control law is the same defined in Equation 8a while the inner loop control law is a 2-DOF PID controller, defined as follows:

$$\begin{aligned} T_c(s) = & \left( K_p + \frac{K_i}{s} \right) (\Omega_v(s) - \Omega(s)) \\ & + \frac{K_d s}{T_f s + 1} (-\Omega(s)) \end{aligned} \quad (11)$$

where  $T_c(s)$ ,  $\Omega_v(s)$  and  $\Omega(s)$  are respectively the Laplace transform related to the  $\tau_c$ ,  $\omega_v$  and  $\omega$ ;  $K_p, K_i$  and  $K_d$  are tuning diagonal 3-by-3 matrixes, while  $T_f$  is the time bandwidth of the filter for the derivative action.

### 3.2. Command filtering

For a UAV quadrotor, the computation of the desired angular velocity, required in the control law (9a), is important to improve the tracking performance, as will be shown in the experimental results. Such a computation can be done analytically starting from the desired rotation matrix  $R_d$ , but this approach can be convoluted if the position controller's expression is complicated. A possible solution can be a command filter (see [6]). Let  $R_d^f$  and  $\omega_d^f$  be, respectively, the filtered desired attitude and angular velocity, then it is possible to define the following second-order command filter:

$$\begin{cases} \dot{R}_d^f = R_d^f S(\omega_d^f) & (12a) \\ \dot{\omega}_d^f = -\omega_n^2 S^{-1}(\text{skew}(R_e)) - 2\xi\omega_n\omega_d^f & (12b) \end{cases}$$

where:

$$R_e^f = R_d^T R_d^f \quad (13)$$

$\omega_n$  is the natural frequency of the filter, while the  $\xi$  is the damping ratio.

## 4. Systematic tuning of nonlinear attitude controllers

This section presents a systematic approach to tune the controller's gain. After showing the linearized version equations presented in Section 3, a general formulation can be state for the tuning of the gains, leveraging the  $H_\infty$  control for the model of a rigid body (2) and finally, a synthesis approach for UAV is derived to find the optimal gains used for simulation/experiments.

### 4.1. Linearized equations

Assume that the point of equilibrium for a generic rigid body is  $R = I_3$  and  $\omega = 0$ , then the rotation matrix around the equilibrium can be approximated, thanks to the Rodrigues' formula, as:

$$R_u(\theta) = I_3 + S(\hat{\theta}). \quad (14)$$

where  $\hat{\theta} \in \mathbb{R}^3$  is the vector of small rotation angles about  $R = I_3$ . The linearized attitude and angular velocity errors are defined as:

$$\begin{cases} \hat{\theta}_e = -(\hat{\theta}_d - \hat{\theta}) = -\bar{\theta}_e, & (15) \\ \omega_e = \omega_v - \omega & (16) \end{cases}$$

The linearized attitude motion is written as:

$$\begin{cases} \dot{\hat{\theta}} = \omega, & (17a) \\ J\dot{\omega} = \tau_c + \tau_e & (17b) \end{cases}$$

with  $J\dot{\omega}$  is substituted by  $\mathbf{G}(s)\omega$  in equation (17b), when UAV quadrotor attitude dynamics is considered.

Thanks to the above derivations, it is possible now to linearize the control law in the function of the variables defined in (15) and (16). The outer loop stabilizer becomes:

$$\begin{cases} \omega_v = \bar{K}_R \bar{\theta}_e + \omega_d & (18a) \\ \dot{\omega}_v = \bar{K}_R \bar{\omega}_e + \dot{\omega}_d & (18b) \end{cases}$$

where,  $\bar{\omega}_e = \omega_d - \omega$  and  $\bar{K}_R = \frac{1}{2}(\text{tr}(K_R)I_3 - K_R)$ . The linearized equations (9a) are:

$$\begin{cases} \dot{\hat{\theta}}_e = -\bar{K}_R \bar{\theta}_e + \omega_e & (19a) \\ J\dot{\omega}_e = -C_c x_c - (D_c + K_\omega)\omega_e - \tau_e & (19b) \\ \dot{x}_c = A_c x_c + B_c \omega_e & (19c) \end{cases}$$

### 4.2. $H_\infty$ synthesis approach

The mixed-sensitivity  $H_\infty$  approach is used to tune the gains of the linearized equations, in order to track properly the setpoint, together with performances and control effort requirements. Along each axis, the linearized dynamics of a rigid body can be written in Laplace form as follows:

$$G(s) = \frac{Q(s)}{\tau_C(s)} = \frac{1}{Js} \quad (20)$$

Assuming that the angular velocity and acceleration are null and a disturbance  $d(t)$  is added after the kinematic Equation (17a), the perturbed angle and angular velocity errors are defined as:

$$\bar{\theta}_{e,pt} = \bar{\theta}_e - d \quad (21a)$$

$$\omega_{e,pt} = \omega_e - \bar{K}_R d \quad (21b)$$

By letting  $A_c = D_c = \mathbf{0}$ ,  $B_c = I_3$  and  $C_c = K_I$ ; it is possible to write the equations in the classic formulation, such as follows:

$$\begin{cases} \omega_v = \bar{K}_R (\bar{\theta} - d) & (22a) \\ J\dot{\omega} = -J(\bar{K}_R \omega) + K_I x_c + K_\omega \omega_{e,pt} & (22b) \\ \dot{\hat{\theta}} = \omega & (22c) \\ \dot{x}_c = \omega_{e,pt} & (22d) \end{cases}$$

For a generic axis, define  $W_S$  and  $W_R$  respectively (using the MATLAB function "makeweight") as the weighting function for performance (to tune the transfer function from  $d$  to  $\omega_{e,pt}$ ) and control effort (to tune the transfer function from  $d$  to  $\tau_c$ ) and consider the following vector of tunable parameters:

$$\rho = [\bar{K}_R, K_I, K_\omega]^T \quad (23)$$

Let  $S(s, \rho)$  and  $R(s, \rho)$  be respectively the sensitivity and control sensitivity transfer function for the classic formulation defined in equation (22). Let the cost related to performance and control requirements be defined as:

$$\begin{cases} J_S(\rho) = \|W_S^{-1}(s)S(s, \rho)\|_\infty & (24a) \\ J_R(\rho) = \|W_R^{-1}(s)R(s, \rho)\|_\infty & (24b) \end{cases}$$

Then, it is possible to state the synthesis problem as an optimization problem:

$$\rho^* = \arg \min_{\rho} J_S(\rho) \quad (25)$$

subject to

$$J_R(\rho) \leq 1 \quad (26)$$

where  $\rho^*$  is the optimal value of the controller gain vector. An equivalent tuning solution can be found by analyzing the equations for error formulation defined as,

$$\begin{cases} \dot{\bar{\theta}}_e = -\bar{K}_R \bar{\theta}_e + \omega_e & (27a) \\ J\dot{\omega}_e = -K_I x_c - K_\omega(\omega_e - \bar{K}_R d) & (27b) \\ \dot{x}_c = \omega_e - \bar{K}_R d & (27c) \end{cases}$$

Indeed, it can be proved that the classic formulation (22) and the error formulation defined by (27) are equivalent and they lead to the same optimal gains.

### 4.3. UAV formulation

The tuning technique can be used for UAV control by first solving the synthesis approach for an inner loop problem where the transfer function  $\mathbf{G}(s)$  and PID-2 defined in equation (11). Let us consider a weighting function  $W_{S,inner}$  for the sensitivity function, but this time, relating  $\omega_v \rightarrow \omega_e$  and consider the following vector of gain parameters:

$$\rho_{inner} = [K_p, K_i, K_d, T_f]^T. \quad (28)$$

It is possible to define the inner loop performance cost  $J_{S,inner}$ :

$$J_{S,inner}(s, \rho_{inner}) = \|W_{S,inner}(s)S_{inner}(\rho_{inner}, s)\|_\infty \quad (29)$$

where  $S_{inner}$  is the sensitivity transfer function with input  $\omega_v$  and  $\omega_e$  as output. Under these definitions, it is possible to state the optimization problem for the inner loop control as follows:

$$\text{Find } \rho_{inner}^* \text{ such that } J_{S,inner} \leq 1 \quad (30)$$

The outer-loop system is defined by equations (17a),(18a) and the inner-loop; the latter is considered to be much more faster than the outer-loop, so when the outer-loop starts its transient, the inner-loop is already at the steady-state value. Thanks to this, the outer loop can be considered without exploiting the inner-loop structure; this results in a simpler tuning of  $\bar{K}_R$ , which can be managed by hand.  $\bar{K}_R$  is the linearized outer loop gain, in order to pass to the non linear gain  $K_R$ , it is necessary to make the following computation:

$$\begin{bmatrix} K_{R1} \\ K_{R2} \\ K_{R3} \end{bmatrix} = \begin{bmatrix} -1 & 1 & 1 \\ 1 & -1 & 1 \\ 1 & 1 & -1 \end{bmatrix} \begin{bmatrix} \bar{K}_{R1} \\ \bar{K}_{R2} \\ \bar{K}_{R3} \end{bmatrix}$$

## 5. Hierarchical attitude control with geodesic feedback

This section presents the attitude control problem solved using the geodesic feedback law, inspired by [4]. The considered design is appealing for UAV attitude control as it allows prioritizing thrust-axis control over yaw direction control, thereby avoiding the risk of propellers saturation due to the poor yaw-torque generation mechanism in quadrotor UAV.

### 5.1. Geodesic feedback formulation

Let  $e_1 \in \mathbb{S}^2$  be a vector expressed in the body-fixed frame on a 3-dimensional rigid body. The reduced attitude vector  $r \in \mathbb{S}^2$  is defined as the inertial frame coordinates of  $e_1$ , which can be written as follows:

$$r = R e_1. \quad (31)$$

Similarly, the reduced attitude error is defined as:

$$r_e = R_e e_1 \quad (32)$$

The reduced error dynamics can be written as:

$$\dot{r}_e = U r_e, \quad (33)$$

where  $U \in so(3)$  is defined as  $R_d^T S(\omega - \omega_d) R_d$ . The reduced attitude stabilization problem aims to design a control input  $u$  to stabilize  $e_1$ . In case of a constant  $v \in \mathbb{S}^3$ , if  $u = v$ , then the dynamics defined in (33) moves  $r_e$  in the steepest descent direction of the geodesic distance  $\theta(v, r_e) = \arccos(v^T r_e)$ ,

$$\arg \min_{u \in \mathbb{S}^3} \dot{\theta} = v \quad (34)$$

When the system is controlled along a path of minimum length in the state space (a great circle in this case),  $u$  said to be geodesic. When moving to the full attitude stabilization,  $U$  is designed such that  $I_3$  is an almost globally asymptotically stable equilibrium (see [1]) of the full attitude  $R_e$ , while the reduced attitude  $r_e$  moves toward  $e_1$  along a great circle. The geodesic feedback law, proposed in [4], is defined as follows,

$$U = P R_e^T - R_e P + k [R_e Q (R_e^T - R_e) Q R_e^T] \quad (35)$$

The first skew-symmetric difference in equation (35) is designed to steer  $R_e P$  to  $P$ , while, when  $\|R_e P - P\|_2$  is small, the second difference kicks in to steer  $R_e Q$  to  $Q$ ; in simple terms, there is a stabilization on  $\mathbb{S}^2$  followed by stabilization on  $SO(3)$ , the two terms are fused into one smooth function.  $k$  presents a trade-off between the reduced and full attitude convergence rates.

To have more freedom in tuning this control law, the following modified formulation is considered:

$$S(\gamma_{R,geo}) = k_2 (R_e^T P - P R_e) + k(\Psi) [Q (R_e^T - R_e) Q], \quad (36)$$

where  $k_2 \in (0, \infty)$  is a gain that weighs the effect of the reduced attitude control, while  $k(\Psi)$  is a parameter variant gain to ensure that for large angle  $\theta$  (the angle between  $r_e$  and the  $e_1$  axis) the

gain is small so that the reduce attitude control is prioritized. The gain function is specifically defined as follows:

$$k(\Psi) = k_{max}(1 - \Psi)^n + k_{min} \Psi^n \quad (37)$$

where  $k_{min}$  and  $k_{max}$  are defined, respectively, as the minimum and the maximum value that  $k(\Psi)$  can assume; and  $\Psi$  is defined as,

$$\Psi = \frac{1 - \cos(\theta)}{2} \quad (38a)$$

$$\cos(\theta) = r_e^T e_1 \quad (38b)$$

Note that to implement the control law within the hierarchical design presented in Section 3, the term  $\dot{\gamma}_v$  in equation 6b must also be evaluated. To this end, the time derivative of  $\gamma_{R,geo}$  can be computed as follows:

$$S(\dot{\gamma}_{R,geo}) = k_2 (\dot{R}_e^T P - P \dot{R}_e) + k(\Psi) Q (R_e^T - R_e) Q + \dot{k}(\Psi) Q (\dot{R}_e^T - \dot{R}_e) Q \quad (39)$$

where,

$$\begin{cases} \dot{k}(\Psi) = -n(1 - \Psi)^{n-1} k_{max} \dot{\Psi} + n \Psi^{n-1} k_{min} \dot{\Psi} \\ \dot{\Psi} = \frac{\sin(\theta)}{2} = \dot{r}_e^T e_1 \end{cases} \quad (40a)$$

$$(40b)$$

## 6. Simulation and Experimental results

This section deals with simulation on the non-linear UAV simulator and the experiments; in the thesis work, a numerical example for the hierarchical control of a rigid body model can be found, that makes use of the hierarchical control law developed so far.

### 6.1. Tuning of the gains

The tuning of the inner loop controller is made, for all three axis, using only the sensitivity transfer function  $S_{inner}$  (that links  $\omega_v$  and  $\omega_e$ ), without using a control effort weighting function, because by choosing carefully the parameters introduced in table 1.

The result coming from the tuning of the gains  $H_\infty$  synthesis, using properly defined transfer function for each axis, introduced in (30), are



	$K_p$	$K_i$	$K_d$	$T_f$
<b>roll</b>	0.046	0.038	$10^{-3}$	108.76
<b>pitch</b>	0.046	0.024	$10^{-3}$	104.67
<b>yaw</b>	0.077	0.32	$1.5 \cdot 10^{-3}$	99.82

Table 1: Gain tuned for inner-loop PID

while, the outer loop control gains are chosen by hand and they are defined as  $\bar{K}_R$  equal to 10, 10 and 3, respectively for the roll, pitch and yaw axis.

## 6.2. UAV software simulations

Simulations are carried out first using the hierarchical classic control law, confronting in different scenarios, in particular a circular trajectory with angular frequency  $\Omega = 1.5 \text{ rad/s}$  and  $\Omega = 2.5 \text{ rad/s}$ ; for each scenario, the results with and without the feedforward term, using as natural frequency  $\omega_n = 20 \text{ rad/s}$  and  $\xi = 1$  in the command filter.

The results coming from this experiment are reported in table 2, where  $\mu_{norm,error}$  (which is the mean value of the norm of the angle error) computed, for each experiments, in Table 2:

	$\Omega = 1.5 \text{ rad/s}$	$\Omega = 2.5 \text{ rad/s}$
<b>feedforward</b>	0.83	3.61
<b>not feedforward</b>	1.70	9.1

Table 2: Mean of the angle norm error [cm]

Regarding the Geodesic control law, the feedforward term will act only for the first two angular velocity term components, while the third is considered to be zero; this is because the third axis must acts only as the geodesic controller, without any other input (in this case, the feedforward term).

The second trajectory, inspired by [5], is defined as:

$$\begin{cases} y_d(t) = 4 \text{ step}(t-1) \text{ m} \\ z_d(t) = -2 \text{ step}(t-1) \text{ m} \\ \psi_d(t) = \hat{\psi} \text{ step}(t-1) \text{ deg} \end{cases} \quad (41)$$

$\hat{\psi}$  first be set to  $30 \text{ deg}$ , and it is tested both using hierarchical and geodesic; then, the same test will be done, but using a larger angle, to better emphasize saturation effects and how the

two systems reacts differently, in front of windup effects, setting  $\hat{\psi}$  equal to  $120 \text{ deg}$ .

The gains used for this experiment are:  $k_{max} = 3$ ,  $k_{min} = 0.01$  and  $k_2 = 5$ ; the natural frequency  $\omega_n$  is now set to  $30 \text{ rad/s}$ . The overshoot percentage of the yaw error is computed for all four cases:

	$\hat{\psi} = 30 \text{ deg}$	$\hat{\psi} = 120 \text{ deg}$
<b>Hierarchical</b>	22.92	32.64
<b>Geodesic</b>	4.64	5.57

Table 3: Overshoot percentage of yaw step response

showing a significant improvement of the performance when considering the geodesic approach.

## 6.3. Experiments

The same experiment done in the Simulation is presented here for a real case scenario, but it is tested first at  $\Omega = 2 \text{ rad/s}$ , the plot of the norm of the position error for this experiment is the following:

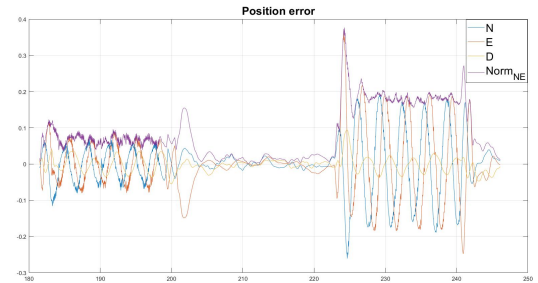


Figure 1: First Experiment Hierarchical (position error)

while, for a circular trajectory at  $\Omega = 2.5 \text{ rad/s}$ ,

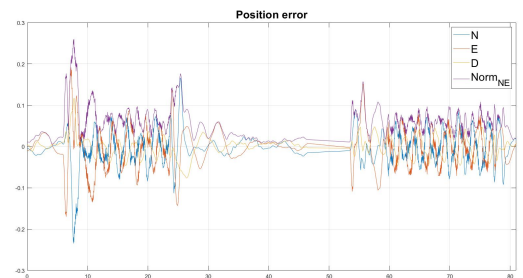


Figure 2: Second Experiment Hierarchical (Attitude angle response)

Regarding the geodesic control law, the more relevant result has been detected by looking at the yaw response for  $135\text{ deg}$ .

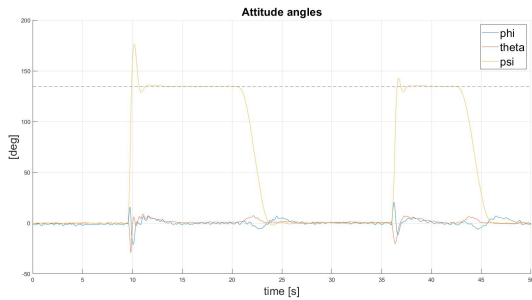


Figure 3: Geodesic vs. Hierarchical (attitude angle response)

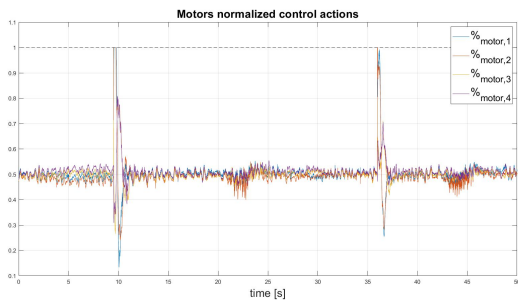


Figure 4: Geodesic vs. Hierarchical (thrust propellers percentage)

## 7. Conclusions

The focus of the thesis is the application of hierarchical attitude control laws to UAVs. Specifically, the hierarchical architecture is implemented within the position control architecture for trajectory tracking in vectored-thrust UAVs by including a nonlinear geometric filter, that allows to easily include feedforward terms to improve tracking performance.

To tune the gains of the control law, the thesis employs the  $H_\infty$  synthesis approach proposed in [3]. The nonlinear equations defining the closed-loop system of the tracking error dynamics are first linearized. This leads to a formulation that is different from the classic one used in  $H_\infty$  synthesis. The method is initially introduced for the ideal rigid body problem and then adapted to address the UAV case.

In the final part of the thesis, a geodesic control law inspired by [4], is implemented within the proposed hierarchical architecture. The control law proposed in [4] has then been modified

to incorporate an error-dependent variable gain, which allows us to effectively prioritize reduced attitude stabilization when the reduced attitude error is large. Simulation and experimental results confirm the benefit of the geodesic stabilizer against a popular nonlinear stabilizer in reducing directionality windup issues associated with propellers saturation.

## References

- [1] D. Angeli. An almost global notion of input-to-state stability. *IEEE Transactions on Automatic Control*, 49(6):866–874, 2004.
- [2] Davide Invernizzi, Marco Lovera, and Luca Zaccarian. Hierarchical dynamic control for robust attitude tracking. *IFAC-PapersOnLine*, 53(2):6171–6176, 2020.
- [3] Davide Invernizzi, Simone Panza, and Marco Lovera. Robust tuning of geometric attitude controllers for multirotor unmanned aerial vehicles. *Journal of Guidance, Control, and Dynamics*, 43(7):1332–1343, 2020.
- [4] Johan Markdahl, Jens Hoppe, Lin Wang, and Xiaoming Hu. A geodesic feedback law to decouple the full and reduced attitude. *Systems & Control Letters*, 102:32–41, 2017.
- [5] Francesco Marzagalli, Pietro Ghignoni, Giovanni Gozzini, and Davide Invernizzi. Experimental validation of an anti-windup design trading off position and heading direction control performance for quadrotor uavs. *IFAC-PapersOnLine*, 55(22):117–122, 2022. 22nd IFAC Symposium on Automatic Control in Aerospace ACA 2022.
- [6] Sheng Zhao, Wenjie Dong, and Jay A Farrell. Quaternion-based trajectory tracking control of vtol-uavs using command filtered backstepping. In *2013 American Control Conference*, pages 1018–1023. IEEE, 2013.